Studying the Growth of Cubic Boron Nitride on Amorphous Tetrahedral Carbon Interlayers

Kar Man Leung, Chit Yiu Chan, Yat Ming Chong, Yuen Yao, Kwok Leung Ma, Igor Bello,* Wen Jun Zhang, and Shuit Tong Lee

Center Of Super-Diamond and Advanced Films (COSDAF) & Department of Physics and Materials Science, City University of Hong Kong, Kowloon Tong, Hong Kong SAR, China

Received: April 1, 2005; In Final Form: July 5, 2005

The growth of cubic boron nitride (cBN) films on bare silicon and amorphous tetrahedral carbon (ta-C) layers prepared on silicon substrates was studied. The cBN films were prepared by radio frequency magnetron sputter deposition at ~870 °C. The original ta-C interlayers were graphitized and restructured under high temperature and possibly under ion bombardment during BN deposition. The majority of graphitic basal planes were nearly perpendicular to the surface of silicon substrates. The BN films grown on these restructured carbon layers were deposited with higher content of cubic phase and did not show delamination signs. Turbostratic BN (tBN) basal planes extended carbon basal planes and their edges served as cBN nucleation sites. The cBN films grown on textured ta-C interlayers were insensitive to the ambient environment. The residual sp^3-bonded carbon phase confined in the interlayers probably acts as a diffusion barrier preventing the oxidation of dangling bonds near BN interface and thus precludes weakening the interface as a result of volume expansion. The carbon interlayers also improve the crystallinity of the oriented tBN because they are continuation of carbon graphitic basal planes so that the volume fraction of nitrogen-void (N-void) defects in the sp^2-bonded BN intermediate layers is reduced. The strong sp^3-bonded carbon matrix could thereto withstand large compressive stress and facilitates deposition of thicker cBN films.

1. Introduction

Cubic boron nitride (cBN) is a compound material with outstanding mechanical and electronic properties. Cubic BN is the material with the second highest hardness, elastic modulus, and thermal conductivity next to diamond. It is, however, superior to diamond in higher graphitization and oxidation temperatures and chemical inertness to molten ferrous materials.[1−5] These properties make it the best material for mechanical applications involving steels and all ferrous materials. Cubic BN is also a potential candidate for construction of high-power and high-speed electronic devices because of its high thermal conductivity and electronic properties which include wide band gap (~6.2 eV), expected high carrier mobility, and doping capacity for both n- and p-type conductivity,[6,7] while n-type doping of competitive diamond is still questionable. However, the incompatibility of cBN with many types of substrates primarily in their physical properties and the process of synthesis is the principal reason of poor cBN film properties including sensitivity to humidity, excessive stress, and delamination of films thicker than 200 nm.[8−10]

Cubic BN often nucleates on an oriented turbostratic boron nitride (tBN) layer[11] grown on a thin amorphous boron nitride (aBN) layer interfacing the substrate.[12] Both cBN nucleation and growth are, however, assisted with energetic ions inducing significant compressive stress which accumulates with the increase in film thickness and leads to instantaneous pealing off of the film upon its exposure to ambient environment or even during deposition when the film thickness is over several hundreds nanometers. The existence of the soft sp^2-bonded interfacial layer aggravates delamination at the interface since tBN/aBN precursor layer is the weakest link between the cBN and substrate.[13]

Considerable effort was made to maximize the thickness of cBN films via stress reduction using a two-step growth,[9] deposition at elevated temperatures (≥900 °C),[10] postdeposition annealing,[14] and postdeposition high-energy ion irradiation.[15] Enhancement of adhesion was also exercised through tailoring the mechanical linkage between the cBN and its underlying substrates by inserting buffer layers. This includes incorporation of β-SiC interlayers,[16] stoichiometricly graded (BN_x) interface layers,[17−19] tensile BN buffer layers,[20] B−C−N gradient layers,[21] AlN interlayers,[22] thick sp^2 buffer layers,[23] Zr-rich composite layers,[24] and so forth. The improvement in film adhesion is usually obtained because of sharing stress by a buffer layer or forming a stronger bonding between the buffer layers and an sp^2-bonded BN interfacial layer. Diamond interlayer was demonstrated to be the best buffer layer for growing thick and adherent cBN films[25] owing to the similarities in their lattice structures (the lattice constants of cBN and diamond are 3.62 and 3.56 Å, respectively),[26] surface energies, and other physical parameters. Epitaxy of cBN directly on AlN[27] and particularly diamond without precursor layers was recently reported[28−31] to be an important step to the synthesis of device quality cBN.

In this work, we have studied growing cBN on another class of carbon materials, incorporated as interlayers, and have investigated their influence on cBN properties. The interlayers were amorphous tetrahedral carbon (ta-C) films, which were graphitized and restructured because of high-deposition temperature and possibly because of ion bombardment during cBN growth. These interlayer materials are termed "ta-C" films in this paper. Most of the graphitic basal planes were aligned nearly

* Author to whom correspondence should be addressed. E-mail: apibello@cityu.edu.hk.

10.1021/jp051656n CCC: $30.25
Published on Web 08/10/2005

in the perpendicular direction to the substrate. Cubic BN with (111) planes (interplanar spacing of 2.09 Å) usually nucleates and grows via 2:3 lattice matching on the edges of (0002) tBN planes with an interplanar spacing of 3.33 Å.[4,32−34] In this case, the tBN can easily be oriented and can extend the aligned graphitic planes of the carbon interlayer. The structural similarity of tBN and aligned graphitic planes probably plays an important role in controlling the cBN nucleation. Mirkarimi et al.[35] reported that high-phase purity of cBN films could be obtained on hard amorphous carbon (a-C) substrates, but the reasons have not been elucidated. This article qualitatively and quantitatively explains the effects of using ta-C coated Si substrates on the cBN content and film adhesion in reference to cBN films grown on bare Si substrates.

2. Experimental Methods

Amorphous tetrahedral carbon (ta-C) interlayers were prepared on Si substrates at the −100 eV bias and ∼60 °C using a filtered cathodic vacuum arc (FCVA) deposition. Deposition details are described elsewhere.[36] Boron nitride films were then grown on the ta-C films employing a radio frequency (RF) magnetron sputter deposition. The base pressure in the deposition chamber was about 10^{-10} Torr. The sputter target disk with 3 in. in diameter was 99.99% pure hexagonal boron nitride (hBN). The sputtering was carried out in argon/nitrogen gas mixtures at a ratio of 2:1 ($Ar:N_2$) with a total gas flow rate of 30 sccm. The deposition pressure was about 16 mTorr. Plasma was induced at the 250 W RF (13.56 MHz) power supplied to the hBN target. The substrate was biased by a high-frequency (HF) power supply operating at 333 kHz. Altering the HF voltage amplitude induced variable DC bias ranging from −60 to −120 V. In each deposition, a ta-C coated Si substrate and p-type (100) bare Si substrate of equal sizes (15 × 10 mm^2) were installed on a molybdenum holder and were loaded into the deposition chamber. The target-to-substrate distance was about 9 cm. Simultaneous growth of cBN on both types of the substrates ensured equal deposition conditions and enabled to deduce the role of the carbon interlayer at cBN growth. The samples were heated to ∼870 °C during deposition using a boralectric BN heater. The substrate temperature was monitored by two K-type thermocouples in different locations of the substrate holder and by an optical pyrometer. The substrates were cleaned in situ by thermal desorption at temperature of ∼870 °C. Sputter cleaning of substrates was not applied to avoid atomic displacement induced by energetic ion bombardment in the surface regions of carbon films.

The phase identification and contents of BN films were obtained from Fourier transform infrared (FTIR) spectroscopic analysis using a PC 1600, Perkin-Elmer FTIR instrument. The microstructures of BN film, ta-C interlayer, and their interfaces were investigated by cross-sectional transmission electron microscopy (XTEM) employing a Philips CM 200 FEG microscope. The cross-sectional morphology and film thickness were investigated by a Philips XL 30 FEG scanning electron microscope (SEM). In addition, a Renishaw Raman system 2000 was used to characterize the phase structures of ta-C interlayers before and after BN deposition.

3. Results and Discussion

Boron nitride films were codeposited on ta-C coated and bare Si substrates at a series of substrate bias voltages. The FTIR spectra obtained from the two substrates after deposition are compared and shown in Figure 1. Three FTIR absorption peaks are usually observed in BN films. The peak centered at ∼1065 cm^{-1} represents the vibrational transverse optical (TO) phonon mode[37] characteristic to cBN. This peak can upshift or downshift to wavenumbers of over 1100 or 1056 cm^{-1}, respectively, depending on the stress level built up inside the film. Hexagonal BN and poorly crystalline sp^2-bonded tBN show peaks positioned at ∼1380 cm^{-1}, representing the B−N stretching within basal planes, and at ∼780 cm^{-1}, representing the B−N−B bending between the basal planes. The cBN volume fractions in BN films on both substrates were estimated from the FTIR absorption peak intensities at wavenumbers of approximately 1080 and 1380 cm^{-1}, labeled as I_{cBN} and $I_{hBN(stretching)}$, respectively, using the expression of $X_{cBN} = I_{cBN}/(I_{cBN} + I_{hBN(stretching)})$.[38]

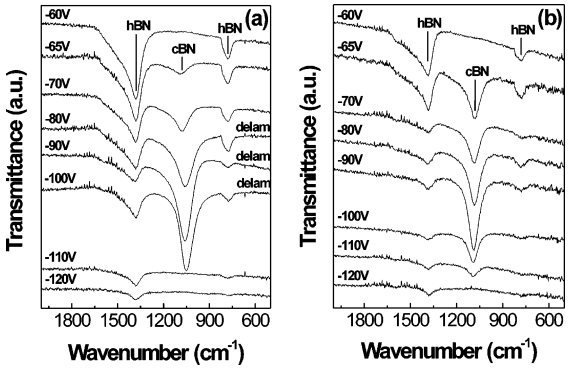

Figure 1. FTIR spectra of BN films deposited on (a) bare Si and (b) ta-C coated substrates at 870 °C for 3 h at different bias voltages.

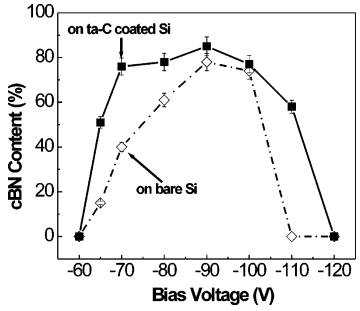

Figure 2. Contents of cubic phase in BN films deposited on bare Si and ta-C coated substrates differ upon the bias voltage used.

The cBN volume fractions on two substrates are calculated and plotted against the bias voltage in Figure 2. Ion energy corresponding to the bias voltage of −65V was the threshold value for cBN nucleation on both substrates at our system configuration. Below this value, only hBN films were deposited. The BN films grown on bare Si substrates at biases from −80 to −100 V tended to delaminate after their air exposure. They are denoted "delam" near the corresponding FTIR spectra in Figure 1a. The films prepared at higher bias voltage delaminate earlier upon air exposure and their cBN peaks in FTIR spectra are downshifted to lower wavelengths and are broadened. The peak downshift is indicative of the stress relaxation. On the other hand, the peak broadening is caused by the coexistence of several different stress levels, including highly stressed bonding as intact films, partially stressed bonding, and stress-relieved bonding, which contribute to the signals in a wider range of wavenumbers. For totally delaminated films (stress-free state), we observed the cBN peak centered at 1056 cm^{-1} with the largest degree of peak broadening. Unlike bare Si substrates, all BN films grown on ta-C interlayers at series of the same bias voltage showed no sign of delamination after the air exposure. The films stored in a drybox remain intact up to now, being already longer than one year. These films are highly

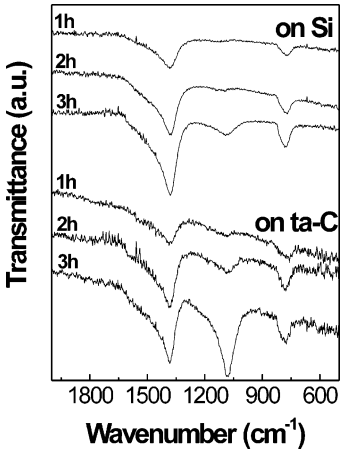

Figure 3. FTIR spectra showing cBN evolution on bare Si and ta-C coated substrates at −65 V and 870 °C illustrated with deposition time of 1−3 h.

stressed as deduced from the cBN peak positions in FTIR spectra. The cBN peaks are centered at wavenumbers higher than 1081 cm^{-1} which are considerable higher values than the value of 1065 cm^{-1} characteristic to cBN crystals synthesized by HPHT methods. The upshift in cBN absorption to higher wavenumbers is more significant with the increase in bias voltage (ion kinetic energy). The film grown at −90 V on ta-C coated Si shows cBN peak centered at wavenumber of 1087 cm^{-1} in Figure 1b with estimated cubic phase volume fraction of ∼85%. The internal compressive stress of this film is larger when compared with cBN rich films deposited by a fluorine-assisted ECR−CVD that yielded cBN TO mode absorption peak[39] at about 1070 cm^{-1}. Using the proportionality of 4 cm^{-1}/GPa as reported by Klett et al.,[40] the difference of 17 cm^{-1} implies that the film presented herein is more compressively stressed in magnitude of 4.25 GPa when compared to that in ref 39. Despite this high stress, cBN films still sustain on ta-C interlayers in contrast to the films with high cBN content grown on bare Si that tended to delaminate at thickness over 200 nm.

Cubic BN films have been deposited on a variety of substrates but with self-forming aBN/tBN precursor layers on many substrates with some exceptions particularly on diamond substrates. The thickness of the precursor layers depends on the energy of ions or bias voltage. Hence, the incubation time for cBN growth prolongs with lowering the particle kinetic energy. Since bias voltage of −65 V was low and close to the nucleation threshold in our system, the incubation period was longer and the sp^2 BN transition layer was thicker than those deposited at higher bias voltages. This can be demonstrated on the evolution of the cBN phase with elapsed deposition time. For example, Figure 3 shows the FTIR spectra of boron nitride films deposited on the two aforementioned substrates at −65 V with deposition time of 1, 2, and 3 h. After 1-h deposition, no cBN absorption peak is observed on bare Si substrate implying that this time is insufficient for cBN incubation. However, a very weak cBN absorption peak is already observed in the spectrum collected from BN films grown on the ta-C/Si substrate indicating that nucleation and early stage of cBN growth starts within 1 h. Two-hour deposition on bare silicon led to a weak sign of an emerging cBN peak, while the deposition on the carbon interlayer yielded the cBN absorption peak being already well resolved. The deposition on bare Si only for time longer than 3 h led to a well distinct cBN peak.

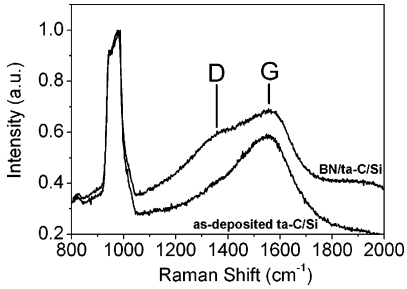

Figure 4. Normalized Raman spectra collected from a ta-C film as-deposited on Si substrate (ta-C/Si) and a restructured ta-C film during BN deposition at 870 °C; second-order silicon peak is at 970 cm^{-1} while BN is not identified because of its nanocrystalline nature.

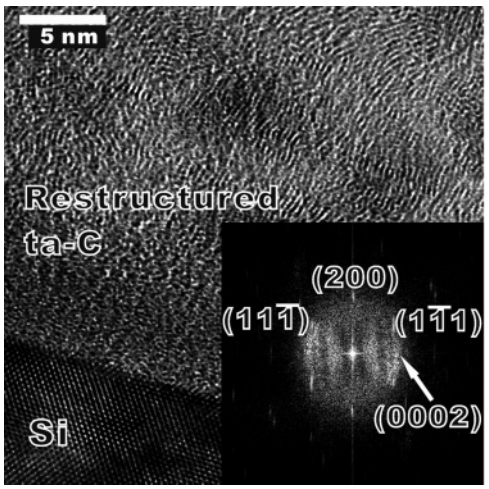

Figure 5. Cross-sectional HRTEM image taken at the restructured ta-C/Si interface. The inset represents FT of the image. In the upper region, the restructured carbon interlayer shows its (0002) graphite planes favorably aligned in the perpendicular direction to the (200) plane of Si substrate as evidenced by FT of the image.

Evidently, incorporation of ta-C interlayer considerably reduces the cBN incubation time in contrast to uncoated bare Si substrates.

The deposition temperature of ∼870 °C causes transformation of ta-C to a partially textured sp^2 carbon layer with graphitic basal planes nearly perpendicular to silicon surface. Ion bombardment during the initial stage of film growth may also have an effect on the texture at the surface-near region. This transformation is revealed in Raman spectra (Figure 4), high-resolution TEM (HRTEM) image, and its Fourier transform (FT) in Figure 5. The phase transformation is consistent with annealing of a-C films at 600 °C reported by McCulloch et al.[41] They explained the preferential orientation of graphitic carbon structures perpendicular to the film surface as consequence of the reduction of strain energy built up in the biaxial stress field. The Raman spectrum in Figure 4 shows graphitization of the ta-C interlayer in a certain extent after cBN deposition, as evidenced by the evolution of short-range disorder peak (D peak). A ta-C coated silicon sample was also annealed at ∼870 °C (without BN deposition) with the same duration as BN deposition and was used as a reference sample. The sample of this control experiment provides similar structural characteristics (not shown) like those obtained from the ta-C films with cBN growth.

Since no cBN Raman signal is detected, the cBN films are nanocrystalline and highly defective.[25] The reduction in incubation time using ta-C interlayer can be explained by the discrepancy in sequential Si/aBN/tBN/cBN and Si/ta-C/tBN/

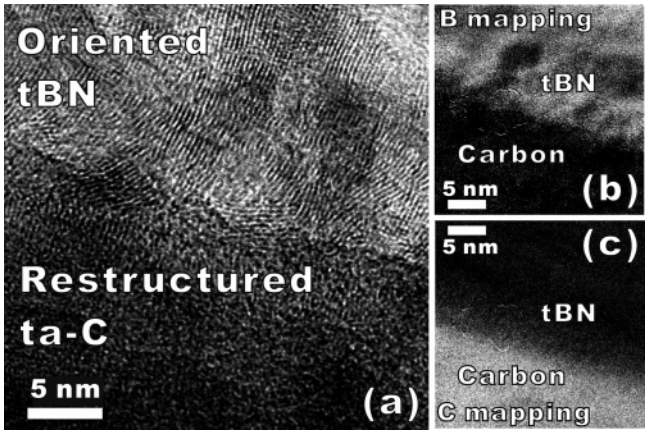

Figure 6. (a) Cross-sectional HRTEM image of the tBN/restructured ta-C interface. Oriented tBN grows directly on restructured ta-C without aBN interface; (b) boron and (c) carbon elemental mapping indicating the BN/carbon interface.

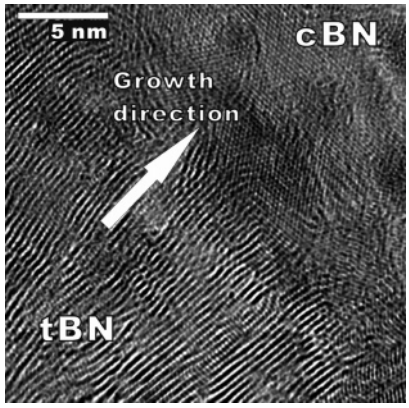

Figure 7. Cross-sectional HRTEM image taken at the cBN/tBN interface. The cBN growth was on a ta-C coated Si substrate.

cBN growth. In both cases, tBN is present and the edges of oriented tBN or curled tBN (0002) planes provide cBN nucleation sites.[8] A time period is required for the formation of aligned tBN on aBN for cBN to furnish nucleation sites. The cBN incubation time is, after all, longer than the time for the aligned tBN formation because the tBN layer is usually grown on an aBN layer. However, deposited amorphous ta-C interlayer is transformed at high-deposition temperature to a carbon structure with similar properties such as those of tBN, and most of the carbon basal planes are extended during BN growth by the equivalent tBN basal planes as seen in the HRTEM image shown in Figure 6a while aBN phase is uneasy to emerge. The restructured ta-C/tBN interface, in Figure 6b and c, visualized by the elemental mapping of boron and carbon, respectively, using electron energy loss spectroscopy (EELS) is lightly diffused in elemental mapping particularly in C mapping. The nonsharp carbon interfacial region is probably induced by carbon diffusion and dynamic recoil ion mixing in an early stage of BN deposition. This depleted carbon region then corresponds to a C−B−N gradient layer, which may participate on the interfacial stress relaxation. The structural similarity of restructured ta-C layer and tBN is probably responsible for favorable and oriented tBN nucleation and growth. The hexagonal graphitic carbon planes are extended by structurally similar tBN planes. Localized areas also indicate emerging oriented tBN directly from amorphous carbon regions as observed in Figure 6a. Since these regions are short-range crystallinity of carbon, it cannot be distinguished whether tBN grows on graphitized sp^2-bonded or sp^3-bonded carbon sites. Turbostratic BN can be formed and aligned faster on the restructured ta-C because these two environments, though chemically different, are structurally equivalent. Therefore, the cBN incubation time is shortened and the sp^2-bonded BN content at the interface between the cBN layer and the substrate is reduced.

In further extent, the enhanced adhesion of cBN on restructured ta-C layer when compared to bare Si can be discussed as follows. The nucleation of cBN is on the edges of oriented tBN in most cases (with exception of some cases especially epitaxial growth on diamond). This is also the case of BN growing on ta-C interlayers as the cross-sectional HRTEM image in Figure 7 illustrates. The tBN (0002) planes are well aligned with the *c* axis parallel to the surface, and they act as cBN nucleation sites. The major difference between using the bare Si and ta-C coated Si substrates is that oriented tBN grows almost directly on restructured ta-C while aBN is an indispensable precursor layer on bare Si substrates. Hence, one of the reasons for the delamination of films grown on bare Si is probably caused by the properties of interfaces particularly those with high density of defects and dangling bonds. Cardinale et al.[42] suggested that diffusion and reaction of water vapor at the film/substrate interface aggravate the film delamination because water weakens the bonding between the film and substrate resulting in adhesion loss. Kim et al.[43] speculated that the film delamination is caused by the volume expansion because of aqueous oxidation reaction with boron dangling bonds, while Jiménez et al.[44] showed that hBN thin films contain nitrogen-void defects in hexagonal bonding using near-edge X-ray-absorption fine structure (NEXAFS) analysis. Accordingly, boron atoms may be bonded to three N atoms, two N atoms, one N atom, or no nitrogen. The diffused carbon region in Figure 6c complements these interpretations but differs from them in substituting void nitrogen atoms by carbon atoms, which strengthened bonding of the BN layer to substrates. Deposition at high temperatures also relieves the stress in both growing BN and originally highly stressed ta-C interlayer. The higher sensitivity and consequential spontaneous delamination of cBN films deposited on bare Si substrates is probably associated with a large number of N-void defects at tBN/aBN/Si regions. The interfacial N-void defects are responsible for boron reactive sites (unsaturated dangling bonds) which in reaction with oxygen and water form unstable oxides and oxyhydrides hampering the film adhesion. The enhanced adhesion is linked with ancillary termination of boron bonds by carbon atoms in interfacial regions which restrict their reactivity. The deposition driven by the dynamic recoil mixing and thermal diffusion aided the termination of active boron sites. Although ta-C films at BN growth conditions are restructured forming a special atomic configuration with oriented graphitic basal planes, the structure is still dense diamondlike carbon (DLC) structure with a considerable density of sp^3 bonding. This dense interfacial carbon in the vicinity of tBN nucleation sites is a good barrier preventing diffusion of oxygen, water, and OH groups, thus forming especially boron oxyhydrides which deteriorate adhesion at sites of B dangling bonds and thus at the BN interface. More importantly, the restructured ta-C system is compatible with tBN systems and therefore enables direct growing of tBN layers with smooth transition of carbon basal planes to BN basal planes reflecting an enhanced interlayer bonding. In other words, the enhanced adhesion of Si/ta-C/tBN/cBN system is also established on the termination of boron dangling bonds and their physical isolation by carbon atoms.

Figure 8 shows the cross-sectional SEM image of cBN film after 6 h deposition on ta-C interlayer at a bias voltage of −80 V with its corresponding FTIR spectrum shown in the inset.

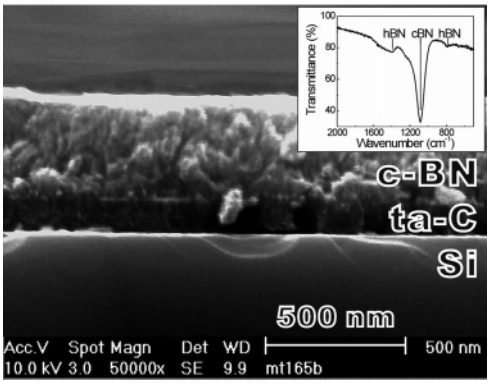

Figure 8. SEM image showing the cross section of a cBN film with thickness of ~350 nm grown on a restructured ta-C interlayer. The inset is the corresponding FTIR spectrum with a narrow cBN TO absorption peak.

The film thickness was approximately 350 nm with high cBN content estimated to be about 86%. The full-width at half-maximum (fwhm) of the TO cBN peak is about 90 cm^{-1}. The typical fwhm value of nanocrystalline cBN films[28] is around 150 cm^{-1}. The BN film with similar thickness (~300 nm) and the cBN content deposited on a B−C−N gradient layer by Yamamoto et al.[45] show fwhm of approximately 200 cm^{-1} which might imply that the higher degree of crystallinity is obtained on the restructured ta-C interlayer. We also deposited BN films on ta-C layers by a two-step process using the biases of −80 and −60 V for cBN nucleation and growth, respectively. The −60 V bias used for cBN growth is already below the cBN nucleation threshold (see Figure 1). The deposition carried out for 3 h yielded TO cBN peak with reduced fwhm (below 80 cm^{-1}), and the peak downshifted to 1079 cm^{-1} while the high cBN content (~80%) was retained. These results imply further improvement in crystalline quality and stress reduction which also is consistent with work carried out by Litvinov et al.[9] who used reduced bias growth.

4. Conclusions

Employing ta-C interlayers enables deposition of more adherent cBN films with higher cBN content and better crystalline quality than on bare Si substrates. The ta-C interlayers are partially transformed at high-deposition temperature in some graphitelike structures with basal planes preferentially oriented in the perpendicular direction to the Si substrates. The ion bombardment during film growth is the second parameter affecting this transformation in the near-surface regions. HRTEM combining with B and C elemental mappings show that oriented tBN tends to grow directly on the restructured ta-C interlayer without intermediate amorphous (aBN) layer unlike the case of bare Si substrates. Thus, the incubation period for cBN nucleation can be reduced using ta-C as interlayers. The cBN films grown on these interlayers are less sensitive to moisture. It is believed that (i) the carbon atoms migrating in dynamic recoil mixing and driven by thermal diffusion process passivate the boron dangling bonds at BN/C interface and (ii) dense sp^3-bonded carbon structure at BN/C interface confines active boron sites and acts as a barrier blocking water and oxygen diffusion into reactive interfacial sites. Thus, it precludes oxidation reaction on dangling bond sites of boron atoms and formation of unstable boron oxide and oxyhydrides that otherwise would inevitably lead to the film delamination. Introducing the structured ta-C interlayer may also improve the crystalline quality of the upper oriented tBN layer because of their structural similarity, which consequently results in reducing N-void defects. The sharp TO cBN peak in FTIR spectrum showing fwhm of smaller than 80 cm^{-1} implies cBN films grow on ta-C interlayers with higher crystalline quality. This work also demonstrates that carbon systems are compatible with BN systems and can be used in many cases of cBN deposition as interlayer to enhance adhesion and functions described above.

Acknowledgment. This work was financially supported by the RGC of Hong Kong SAR under grant No. CityU 1130/04E and CityU 2/04C.

References and Notes

(1) Holleck, H. *J. Vac. Sci. Technol., A* **1986**, *4*, 2661.
(2) Vel, L.; Demazeau, G.; Etourneau, J. *Mater. Sci. Eng., B* **1991**, *10*, 149.
(3) Riedel, R. *Adv. Mater.* **1994**, *6*, 549.
(4) Mirkarimi, P. B.; McCarty, K. F.; Medlin, D. L. *Mater. Sci. Eng.* **1997**, *R 21*, 47.
(5) Zhang, W. J.; Bello, I.; Lifshitz, Y.; Lee, S. T. *MRS Bull.* **2003**, *28*, 184.
(6) Wentorf, R. H., Jr. *J. Chem. Phys.* **1962**, *36*, 1990.
(7) Mishima, O. In *Synthesis and Properties of Boron Nitride*; Pouch, J. J., Alterovitz, S. A., Eds.; Trans Tech Publications: Brookfield, VT, 1990; Vol. 54−55, p 313.
(8) Li, Q.; Marks, L. D.; Lifshitz, Y.; Lee, S. T.; Bello, I. *Phys. Rev. B* **2002**, *65*, 045415.
(9) Litvinov, D.; Clarke, R. *Appl. Phys. Lett.* **1997**, *71*, 1969.
(10) Matsumoto, S.; Zhang, W. J. *Jpn. J. Appl. Phys.* **2002**, *39*, 442.
(11) Li, Q.; Zhou, Z. F.; Lee, C. S.; Lee, S. T.; Bello, I. *Diamond Relat. Mater.* **2001**, *10*, 1886.
(12) Kester, D. J.; Ailey, K. S.; Davis, R. F.; More, K. L. *J. Mater. Res.* **1993**, *8*, 1213.
(13) Reinke, S.; Kuhr, M.; Kulisch, W. *Diamond Relat. Mater.* **1996**, *5*, 508.
(14) Donner, W.; Dosch, H.; Ulrich, S.; Ehrhardt, H.; Abernathy, D. *Appl. Phys. Lett.* **1998**, *73*, 777.
(15) Widmayer, P.; Schwertberger, D.; Wenig, M.; Ziemann, P.; Bergmaier, A.; Dollinger, G. *Diamond Relat. Mater.* **1998**, *7*, 1503.
(16) Mirkarimi, P. B.; Medlin, D. L.; McCarty, K. F. *Appl. Phys. Lett.* **1995**, *66*, 2813.
(17) Freudenstein, R.; Kulisch, W. *Thin Solid Films* **2002**, *132*, 420−421.
(18) Setsuhara, Y.; Kumagai, M.; Suzuki, M.; Suzuki, T.; Miyake, S. *Surf. Coat. Technol.* **1999**, *116*, 100.
(19) Okamoto, M.; Yokoyama, Y.; Osaka, Y. *Jpn. J. Appl. Phys.* **1990**, *29*, 930.
(20) Yap, Y. K.; Aoyama, T.; Wada, Y.; Yoshimura, M.; Mori, Y.; Sasaki, T. *Diamond Relat. Mater.* **2000**, *9*, 592.
(21) Bewilogua, K.; Keunecke, M.; Weigel, K.; Wiemann, E. *Thin Solid Films* **2004**, *86*, 469−470.
(22) Otaño-Rivera, W.; Messier, R.; Pilione, L. J.; Santiago, J. J.; Lamaze, G. *Diamond Relat. Mater.* **2004**, *13*, 1690.
(23) Wong, S. F.; Ong, C. W.; Pang, G. K. H.; Baba-Kishi, K. Z.; Lau, W. M. *J. Vac. Sci. Technol., A* **2004**, *22*, 676.
(24) Wong, S. F., Ong, C. W.; Pang, G. K. H.; Li, Q.; Lau, W. M. *Diamond Relat. Mater.* **2004**, *13*, 1632.
(25) Bello, I.; Chan, C. Y.; Zhang, W. J.; Chong, Y. M.; Leung, K. M.; Lee, S. T.; Lifshitz, Y. *Diamond Relat. Mater.* **2005**, *14*, 1154.
(26) Zhang, W. J.; Bello, I.; Lifshitz, Y.; Chan, K. M.; Wu, Y.; Chan, C. Y.; Meng, X. M.; Lee, S. T. *Appl. Phys. Lett.* **2004**, *85*, 1344.
(27) Felderman, H.; Ronning, C.; Hofsäss, H.; Huang, Y. L.; Seibt, M. *J. Appl. Phys.* **2001**, *90*, 3248.
(28) Zhang, X. W.; Boyen, H.-G.; Deyneka, N.; Ziemann, P.; Banhart, F.; Schreck, M. *Nat. Mater.* **2003**, *2*, 312.
(29) Zhang, W. J.; Bello, I.; Lifshitz, Y.; Chan, K. M.; Wu, Y.; Chan, C. Y.; Meng, X. M.; Lee, S. T. *Adv. Mater.* **2004**, *16*, 1405.
(30) Zhang, W. J.; Bello, I.; Lifshitz, Y.; Chan, K. M.; Wu, Y.; Chan, C. Y. *Appl. Phys. Lett.* **2004**, *8*, 1344.
(31) Zhang, X. W.; Boyen, H.-G.; Ziemann, P.; Banhart, F. *Appl. Phys. A* **2005**, *80*, 735.
(32) Zhou, W. L.; Ikuhara, Y.; Suzuki, T. *Appl. Phys. Lett.* **1995**, *67*, 3551.
(33) Lambrecht, W. R. L.; Lee, C. H.; Segall, B.; Angus, J. C.; Li, Z.; Sunkara, M. *Nature* **1993**, *364*, 607.
(34) Widany, J.; Frauenheim, T.; Lambrecht, W. R. L. *J. Mater. Chem.* **1996**, *6*, 899.

(35) Mirkarimi, P. B.; McCarty, K. F.; Cardinale, G. F.; Medlin, D. L.; Ottesen, D. K.; Johnsen, H. A. *J. Vac. Sci. Technol., A* **1996**, *14*, 251.
(36) Luk, W. Y.; Kutsay, O.; Bello, I.; Lifshitz, Y.; Lam, C. W.; Meng, X.; Lee, S. T. *Diamond Relat. Mater.* **2004**, *13*, 1427.
(37) Gielisse, P. J., Mitra, S. S.; Plendl, J. N.; Griffis, R. D.; Mansur, L. C.; Marshall, R.; Pascoe, E. A. *Phys. Rev.* **1967**, *155*, 1039.
(38) Lu, M.; Bousetta, A.; Sukach, R.; Bensaoula, A.; Walters, K.; Eipers-Smith, K.; Schultz, A. *Appl. Phys. Lett.* **1994**, *64*, 1514.
(39) Chan, C. Y.; Zhang, W. J.; Chan, K. M.; Bello, I.; Lee, S. T. *Chem. Vap. Deposition* **2003**, *9*, 181.
(40) Klett, A.; Freudenstein, R.; Plass, M. F.; Kulisch, W. *Surf. Coat. Technol.* **2000**, *125*, 190.
(41) McCulloch, D. G.; Peng, J. L.; McKenzie, D. R.; Lau, S. P.; Sheeja, D.; Tay, B. K. *Phys. Rev. B* **2004**, *70*, 085406.
(42) Cardinale, G. F.; Mikarimi, P. B.; McCarty, K. F.; Klaus, E. J.; Medlin, D. L.; Clift, W. M.; Howitt, D. G. *Thin Solid Films* **1994**, *253*, 130.
(43) Kim, I.-H.; Kim, S.-H.; Kim, K.-B. *J. Vac. Sci. Technol., A* **1998**, *16*, 2295.
(44) Jiménez, I.; Jankowski, A. F.; Terminello, L. J.; Sutherland, D. G. J.; Carlisle, J. A.; Doll, G. L.; Tong, W. M.; Shuh, D. K.; Himpsel, F. J. *Phys. Rev. B* **1997**, *55*, 12025.
(45) Yamamoto, K.; Keunecke, M.; Bewilogua, K. *Thin Solid Films* **2000**, *331*, 377−378.